Comparison of bio-physical marine products from SeaWiFS, MODIS and a bio-optical model with *in situ* measurements from Northern European waters*

D Blondeau-Patissier, G H Tilstone, V Martinez-Vicente and G F Moore

Plymouth Marine Laboratory, Prospect Place, West Hoe, Plymouth PL1 3DH, UK

E-mail: dbp202@pml.ac.uk, ghti@pml.ac.uk, vmv@pml.ac.uk and gfm@pml.ac.uk

Abstract
In this paper, we compare bio-physical marine products from SeaWiFS, MODIS and a novel bio-optical absorption model with *in situ* measurements of chlorophyll-a (Chla) and total suspended material (TSM) concentrations, normalized water-leaving radiances (nL_w) and absorption coefficients of coloured dissolved organic matter (a_{CDOM}), total particulate (a_{total}) and phytoplankton (a_{phy}) for 26 satellite match-ups in three Northern European seas. Cruises were undertaken in 2002 and 2003 in phytoplankton dominated open ocean waters of the Celtic Sea and optically complex waters of the Western English Channel (WEC) and North Sea. For all environments, Chla concentrations varied from 0.4 to 7.8 mg m^{-3}, TSM from 0.2 to 6.0 mg l^{-1} and a_{CDOM} at 440 nm from 0.02 to 0.30 m^{-1}.

SeaWiFS OC4v4, with the Remote Sensing Data Analysis Service (RSDAS) atmospheric correction for turbid waters, showed the most accurate retrieval of *in situ* Chla (RMS = 0.24; $n = 26$), followed by MODIS chlor_a_3 (RMS = 0.40; $n = 26$). This suggested that improving the atmospheric correction over optically complex waters results in more accurate Chla concentrations compared to those obtained using more complicated Chla algorithms. We found that the SeaWiFS OC4v4 and the MODIS chlor_a_2 switching band ratio algorithms, which mainly use longer wavebands than 443 nm, were less affected by CDOM. They were both more accurate than chlor_MODIS in the higher CDOM waters of the North Sea. Compared to MODIS the absorption model was better at retrieving a_{total} (RMS = 0.39; $n = 78$) and a_{CDOM} (RMS = 0.79; $n = 12$) in all study areas and TSM in the WEC (RMS = 0.04; $n = 10$) but it underestimated Chla concentrations (RMS = 0.45; $n = 26$). The results are discussed in terms of atmospheric correction, sensor characteristics and the functioning and performance of Chla algorithms.

Keywords: ocean colour, MODIS, SeaWiFS, coastal zone, chlorophyll, inherent optical properties

---

1. Introduction

Accurate estimation of ocean colour and associated products in coastal waters has not yet been possible because of the optical complexity of these waters and the limitations of satellite sensors. Coastal regions represent only 10% of the surface area of the global ocean, but account for 30% of the global primary production (Wollast 1998) and have a high commercial importance. Ship borne monitoring programmes are both spatially and temporally limited. Satellite remote sensing therefore offers a powerful tool for regional and global scale monitoring of the spatial distribution of key marine environmental parameters.

The estimates of chlorophyll-a (Chla) concentration in ocean surface waters from the first ocean colour sensor, CZCS, were of poor quality due to its limited capabilities (Hooker *et al* 1993). The next generation of NASA ocean colour sensors, such as SeaWiFS (1997), Terra-MODIS (1999) and more recently Aqua-MODIS (2002), provides a quantitative time series of Chla concentrations due to higher spectral resolution, more stable calibration and more spectral bands. SeaWiFS was designed to provide accurate normalized water-leaving radiance (nL_w) and Chla concentrations in phytoplankton dominated waters, where the absorption of light is closely related to that of phytoplankton (Morel and Prieur 1977, Gordon and Morel 1983). It is assumed in these waters that the other inherent optical constituents have little influence on the upwelling radiance or co-vary with phytoplankton, although this may not always be true (Siegel and Michaels 1996). In optically complex coastal waters, the high total suspended material (TSM) and coloured dissolved organic matter (CDOM) cause a decoupling of phytoplankton absorption and the underwater light field, and the accurate retrieval of Chla is far more complex. Algorithms designed for phytoplankton dominated waters tend to break down in turbid coastal waters because the optical signature of CDOM can mask phytoplankton absorption at 443 nm (Sathyendranath 2000) and therefore different approaches to algorithm parametrization are required. Theoretically, the position and width of bands available for sensors such as MODIS should enhance the atmospheric correction (Esaias *et al* 1998) and may therefore make the accurate determination of Chla concentrations, in CDOM and TSM rich waters, more achievable.

To date, little work has been done on comparing SeaWiFS and MODIS in different environments. Darecki and Stramski (2004) compared SeaWiFS and MODIS algorithms against 932 radiometric and 707 Chla measurements from 25 cruises in the CDOM rich waters of the Baltic Sea. They found that both SeaWiFS OC4v4 and MODIS algorithms showed systematic errors in Chla of >150%, but found that regional parametrization of algorithms improved estimates of Chla, especially for MODIS chlor_a_2. Other novel algorithms are available for the estimation of bio-physical products in turbid waters (e.g. Schiller and Doerffer 1999, Gons 1999, Ruddick *et al* 2000). Moore and Aiken (2004) have developed a fully analytical bio-optical absorption model for the estimation of IOPs and found that in the Atlantic Ocean and the Western English Channel (WEC) it improved estimates of Chla concentrations compared to SeaWiFS OC4v4. This algorithm remains untested in North Sea waters.
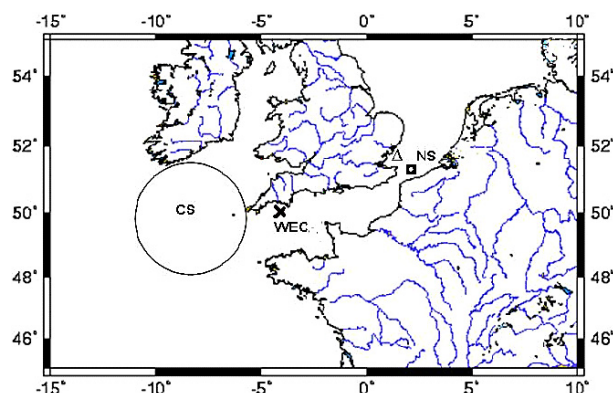
Figure 1. Study areas showing stations sampled in the Celtic Sea (CS; ○), station L4 in the Western English Channel (WEC; ×) and stations along the UK (△) and Belgian (▪) coasts of the North Sea (NS).

Both the WEC and North Sea have relatively shallow depths and high mixing and exhibit a significant input from riverine inflows, which results in different proportions of CDOM (Warnock *et al* 1999) and TSM (Van der Woerd 1999), depending on the time of year and proximity to the coast. These factors make them optically more complex compared to the Celtic Sea which is phytoplankton dominated. The North Sea and surrounding environments are commercially important for the fishery and tourism industries and can be affected by harmful algal blooms and eutrophication (Lancelot *et al* 1987).

In this paper, we assess the performance of MODIS algorithms, SeaWiFS OC4v4 and a bio-optical absorption model coupled with SeaWiFS radiances, at estimating Chla and TSM concentrations, normalized water-leaving radiances (nL_w) and the absorption coefficients of total particulate material, phytoplankton and CDOM in the North Sea, Celtic Sea and WEC. The performance of each algorithm is assessed at basin and regional scales and the results are discussed in terms of atmospheric correction, algorithm parametrization and sensor radiometric accuracy.

2. Material and methods

2.1. Study area characteristics and sampling regime

Bio-optical samples were collected in the Southern WEC in 2002 and 2003 at a frequency of one to two times per week on RV Squila from a monitoring station, 'L4' in Plymouth Sound, located at 50° 15N, 4° 11W. Samples were also collected during one cruise in the Celtic Sea (48–52° N to 1–11° W) on RV Discovery from 1 to 14 April 2002. Two cruises were conducted in the North Sea (51–53° N to 0–4° E), the first from the Belgian coast to the SE coast of the UK from 17 to 21 June 2002 on RV Belgica (cruise BE02-14) and the second on the East coast of the UK (EA 02 cruise) from 25 to 27 June 2002 on RV Water Guardian (figure 1). North Sea stations were typically less than 200 m deep, whereas Celtic Sea stations ranged from 200 to 1000 m.

At each station, discrete samples were collected from Niskin bottles for the determination of HPLC pigments, CDOM and particulate absorption coefficients. *In situ* TSM was only sampled along the Belgian coast of the North Sea
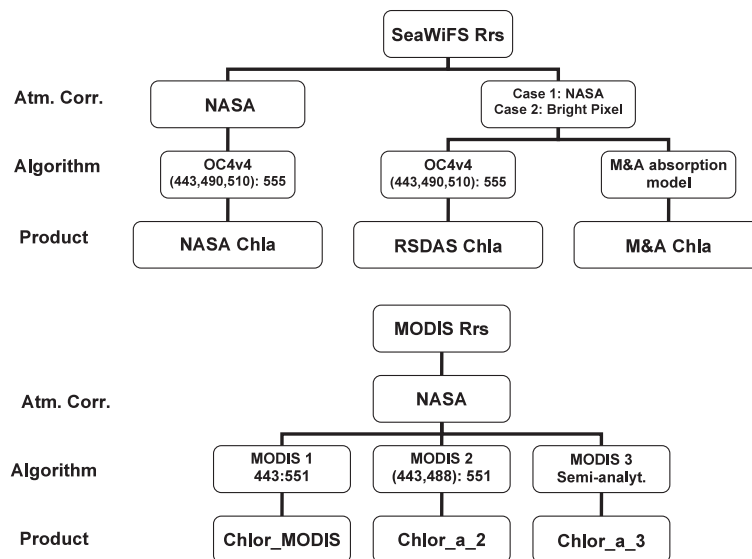
Figure 2. Processing chain used for deriving Chla products from SeaWiFS, MODIS and the Moore and Aiken absorption model.

and in the WEC. Upwelling and downwelling irradiance were measured in the WEC. These field measurements were compared with 26 coincident satellite match-ups from SeaWiFS and MODIS. Satellite overpasses were within 30 min to 4 h of *in situ* sampling time. Abbreviations, symbols and units for each variable are given in appendix A.

2.2. In situ measurements of the bio-physical parameters

2.2.1. Phytoplankton absorption coefficients. The absorption coefficient of total particulate material retained on GF/F filters and detrital matter after pigment extraction using sodium hypochloride (NaClO, 1% active chloride), were determined following the method of Tassan and Ferrari (1995). Three replicates of each sample were frozen on board in liquid nitrogen and absorption coefficients were determined in the laboratory no more than three months after the samples were taken. Spectral measurements were made from 350 to 750 nm at a 1 nm bandwidth using a dual-beam Perkin Elmer Lambda 800 spectrophotometer retro-fitted with a spectralon coated integrating sphere. The spectrophotometer was calibrated using holmium oxide filters every 5 days. The optical density (OD) of the sample was measured in both transmission and reflectance modes and total absorption was determined by removing the contribution of backscattered light (Tassan and Ferrari 1995). Pre-filtered seawater (0.2 μm) was re-filtered through GF/F filters, which were read as blanks. Care was taken that the blank filter side matched the sample filter and after pigment extraction MilliQ water was re-filtered through the GF/F to remove any residual NaClO (Tassan and Ferrari 2002). Correction for pathlength amplification on the filters was carried out using the methods of Tassan and Ferrari (1998) for high TSM waters. The spectral absorption coefficient of phytoplankton was calculated from OD and the ratio of the volume of seawater filtered to the filter area (Tassan and Ferrari 1995).

2.2.2. CDOM absorption coefficients. Replicate seawater samples were taken at the surface and filtered through 0.2 μm

pore size filters (Whatman Nuclepore membranes) using pre-ashed glassware. The first two 250 ml portions of filtered seawater were discarded. The absorption properties of the third sample were determined from 350 to 750 nm using a dual-beam Perkin Elmer Lambda-800 spectrophotometer with no integrating sphere and a 10 cm quartz cuvette, relative to a bi-distilled MilliQ reference blank. Samples from L4 and Cruise D-261 (figure 1) were determined immediately after filtering. Samples from cruises EA02 and BE02-14 were spiked with 0.5 ml of a solution of 10 g l^{-1} of NaN$_3$ per 100 ml of sample to prevent degradation of CDOM (Ferrari *et al* 1996) and stored in a refrigerator for not more than 10 days until analysis (Mitchell *et al* 2000). Baseline corrected optical density (OD) values were multiplied by the ratio of 2.3 to the cuvette path length for each nanometre to calculate the spectral absorption coefficient of CDOM ($a_{\text{CDOM}}(\lambda)$).

2.2.3. High pressure liquid chromatography (HPLC) determination of chlorophyll-a. Chlorophyll-a concentrations were analysed using HPLC with a diode array detection system (Mantoura and Llewellyn 1983). Water samples were filtered through 25 mm GF/F filters and stored in liquid nitrogen. Pigments were extracted with the aid of sonication in 90% acetone, clarified using centrifugation and analysed following the procedure outlined in Barlow *et al* (1997). Pigments were separated using a 3 μm Hypersil MOS2 C8 column on a Thermo Separations product HPLC, detected by absorbance at 440 nm and identified by retention time and on-line diode array spectroscopy.

2.2.4. Total suspended material (TSM). 47 mm GF/F filters were pre-ashed at 450 °C and then pre-washed in 500 ml of MilliQ to remove friable fractions that can be dislodged during filtration. They were then dried in a hot air oven at 75 °C for one hour, pre-weighed and stored in a dessicator with silica gel (Van der Linde 1998, Tilstone *et al* 2004a). A single seawater sample was filtered onto three replicate pre-weighed filters (GF/F membranes; 0.7 μm pore-size) and washed three times with 50 ml MilliQ to remove residual salt. Blanks were also

washed with MilliQ. The filters were weighed on a Sartorius R-200D semi-microbalance (detection limit 10 μg).

2.2.5.   Normalized water-leaving radiance.   In situ above-water downwelling irradiance was measured using a SATLANTIC OCR deck cell and subsurface downwelling irradiance and upwelling radiance were measured using profiling SATLANTIC optical heads in the WEC at station L4 and extrapolated to the surface to calculate above-water reflectance, $\rho_w(\lambda)$, using the approach of Mueller and Austin (1995).   The Satlantic OCR optical heads were calibrated according to SeaWiFS protocols (Mueller *et al* 2000) and were traceable using NIST standards. The normalized water-leaving radiance (nL_w) was calculated as follows:

$$nL_w(\lambda) = \frac{\rho_w(\lambda)}{\pi} f_0(\lambda) \quad \text{(in mW cm}^{-2} \ \mu\text{m}^{-1} \ \text{sr}^{-1})$$

where $f_0(\lambda)$ is the mean extraterrestrial solar irradiance (in mW cm^{-2} μm^{-1}).

For each *in situ* parameter, an inter-calibration was performed at L4 and stations closer to the coast between five European laboratories (Tilstone *et al* 2004b). nL_w was within 5%, HPLC Chla within 9%, the absorption coefficient of phytoplankton within 14% and TSM and CDOM within 20%.

2.3. Description of satellite algorithms and data handling

2.3.1.   The SeaWiFS OC4v4 algorithm.   The SeaWiFS OC4v4 algorithm is a fourth-order polynomial, switching from remote-sensing reflectance (R_{rs}) R_{rs} 443/R_{rs} 555 to R_{rs} 490/R_{rs} 555 and/or R_{rs} 510/R_{rs} 555 using the maximum band ratio depending on the reflectance characteristics of the water type (O'Reilly *et al* 1998, 2000). SeaWiFS can provide two types of images: a full resolution (1.1 × 1.1 km) local area coverage (LAC) and a low resolution (4.4 × 4.4 km) global area coverage (GAC). Full resolution data are transmitted continuously in high resolution picture transmission (HRPT), and were received by Dundee Satellite Receiving station, decoded and transferred to the Remote Sensing Group at Plymouth Marine Laboratory (PML). SeaWiFS level 1 images were processed using the PML software PANORAMA (Lavender and Groom 1999) with RSDAS atmospheric correction (RSDAS ac) which uses the NASA atmospheric correction (NASA ac) for phytoplankton dominated waters and the Bright Pixel atmospheric correction (BP ac) for turbid waters (Moore *et al* 1999).

The RSDAS ac is a pixel-by-pixel atmospheric correction which flags coastal turbid waters depending on their TSM concentrations.   A partitioning between phytoplankton dominated and sediment dominated waters is possible because spectral shapes of $\rho_w(\lambda)$ in the NIR have a sharp threshold at even modest concentrations of TSM (>2 mg l^{-1}; Moore *et al* 1999). The flag for turbid waters is set for a pixel if $L_w(670)$ based on the NASA ac is above a threshold level and the iterative BP ac is triggered.   SeaWiFS OC4v4 Chla concentrations with RSDAS ac were also compared with those using standard NASA ac. The processing chain used for each algorithm is illustrated in figure 2.

2.3.2.   MODIS algorithms.   The match-up data set was only compared with Terra-MODIS data[1].   MODIS offers three Chla products. The standard chlorophyll algorithm for phytoplankton dominated waters is chlor_MODIS (MOD19, parameter 14 (Clark *et al* 1997)), based on the 443:551 band ratio. This algorithm was validated using measurements of Chla (including both the mono- and di-vinyl chlorophylls) from HPLC. The MODIS chlor_a_2 chlorophyll algorithm (MOD21, parameter 26 (Carder *et al* 1999b)) is a SeaWiFS analogue and is intended to be as close as possible to the SeaWiFS chlorophyll standard algorithm.   chlor_a_2 is based on the OC3M algorithm described in the SeaWiFS Post-Launch Technical Memorandum series (O'Reilly *et al* 2000). MODIS chlor_a_3 is specifically designed for optically complex waters. The chlor_a_3 product is based on an inverted semi-analytical, bio-optical model of remote-sensing reflectance, $R_{rs}(\lambda)$. The inversion of a spectral reflectance model is used to solve for chlorophyll in the presence of CDOM and TSM (see Carder *et al* 1999a and figure 2, appendix B).

Terra-MODIS geolocated level 2 (1 km; local scene) ocean data Chla concentrations and absorption coefficient products for 2002 and 2003 match-ups were downloaded from the DAAC[2]. Estimates of the six products were extracted using SeaDAS (Fu *et al* 1998) and compared with the ground truth measurements. MODIS level 2 quality flags were displayed for the six MODIS products. Four different quality flags can be identified: (0) good, (1) questionable, (2) cloudy or (3) bad, although these are not displayed on chlor_a_2. The 26 match-ups were restricted to only good (0) quality flags for the nL_w product since it is a key parameter that determines the accuracy of all other level 2 products. If the nL_w was flagged as good quality, good (0) and questionable (1) flags were used for the other derived products.

2.3.3.   Moore and Aiken bio-optical model.   The Moore and Aiken (2004) bio-optical absorption model, hereafter called the absorption model, calculates the major IOPs for both phytoplankton and CDOM-TSM dominated waters from remotely sensed data and uses the RSDAS ac. The outputs of the model are the concentration of Chla and TSM, a_{CDOM} (443), the total absorption coefficient, a_{total}, at 412, 443, 490, 510 and 555 nm and the backscattering coefficient, $b_b(\lambda)$, at 490 nm. These products are derived from the spectral slopes of absorption ($\varepsilon_{a(\lambda_i, \lambda_j)}$) and backscattering ($\varepsilon_{bb(\lambda_i, \lambda_j)}$), where ($\lambda_i$) and ($\lambda_j$) are 490 and 510 nm respectively. Moore and Aiken (2004) showed that the advantage of using these wavelengths for scaling spectral slopes to give concentrations of the main IOPs is that the standard deviation between these two bands is low. Given $\varepsilon_{a(\lambda_i, \lambda_j)}$ and $\varepsilon_{bb(\lambda_i, \lambda_j)}$, determined from climatology, the model solves $a(\lambda_j)$ and $b_b(\lambda_j)$ for any pair of bands by an iterative loop after three to seven iterations.

The functional forms of the different algorithms and models for SeaWiFS, MODIS and the absorption model are listed in appendix B. *In situ* measurements of Chla and TSM concentration, total absorption coefficient at 412, 443 and 488–490 nm, CDOM absorption coefficient at 400 and

---

[1] http://modis-ocean.gsfc.nasa.gov/parameters.html

[2] MODIS-DAAC: MODIS-Distributed Active Archive Center;
http://acdisx.gsfc.nasa.gov/data/dataset/MODIS/03_Ocean/01_Level2/

Table 1. Range (mean and standard deviation) of TSM, Chl-a, CDOM, a_{tot} and a_{phy} for the different regions. (NS—North Sea, CS—Celtic Sea, WEC—Western English Channel—and nd—no data.)

	Belgica 2002-14 NS, June 2002	Environ. Agency NS, June 2002	D-261 CS, April 2002	L4 time series WEC, 2002, 2003
n	3	4	8	11
TSM (mg l^{-1})	3.63–5.91 (4.44 ± 1.28)	nd	nd	0.25–0.64 (0.39 ± 0.15)
Chla (mg m^{-3})	3.50–7.60 (5.11 ± 2.19)	2.06–3.35 (2.52 ± 0.58)	0.40–7.79 (2.21 ± 0.45)	0.46–2.59 (1.36 ± 0.61)
$a_{CDOM(440)}$ (m^{-1})	0.19–0.30 (0.26 ± 0.06)	0.00–0.02 (0.005 ± 0.004)	1 station (0.05)	0.00–0.05 (0.02 ± 0.02)
a_{total} (m^{-1})	0.07–0.53 (0.30 ± 0.15)	0.04–0.60 (0.23 ± 0.11)	0.01–0.16 (0.08 ± 0.04)	0.00–0.13 (0.05 ± 0.03)
$a_{phy(675)}$ (m^{-1})	0.07–0.19 (0.12 ± 0.06)	0.02–0.04 (0.03 ± 0.01)	0.02–0.08 (0.05 ± 0.04)	0.01–0.05 (0.03 ± 0.02)

Table 2a. Log–log model II regression statistics for chlorophyll-a.

Area	n	Moore and Aiken absorption model with RSDAS ac	SeaWiFS OC4v4 with RSDAS ac	SeaWiFSOC4v4 with NASA ac[a]	chlor_MODIS	chlor_a_2	chlor_a_3
Overall	26	$y = 0.65x - 0.27$ $R^2 = 64\%$	$y = 1.14x - 0.08$ $R^2 = 80\%$	$y = 1.54x - 0.15$ $R^2 = 65\%$	$y = 1.55x - 0.28$ $R^2 = 46\%$	$y = 1.48x - 0.31$ $R^2 = 54\%$	$y = 1.31x - 0.16$ $R^2 = 40\%$
NS	7	$y = 0.94x - 0.33$ $R^2 = 23\%$	$y = 0.73x + 0.32$ $R^2 = 75\%$	$y = -2.02x + 1.92$ $R^2 = 49\%$	$y = -2.47x + 2.00$ $R^2 = 54\%$	$y = -1.91x + 1.66$ $R^2 = 70\%$	$y = -1.93x + 1.71$ $R^2 = 67\%$
CS	8	$y = 0.24x - 0.33$ $R^2 = 81\%$	$y = 0.75x + 0.24$ $R^2 = 91\%$	$y = 0.78x - 0.32$ $R^2 = 93\%$	$y = 0.64x - 0.50$ $R^2 = 66\%$	$y = 0.76x - 0.52$ $R^2 = 75\%$	$y = 0.57x - 0.23$ $R^2 = 66\%$
WEC	11	$y = 0.55x - 0.22$ $R^2 = 59\%$	$y = 0.54x + 0.03$ $R^2 = 88\%$	$y = 0.90x - 0.03$ $R^2 = 71\%$	$y = 0.57x - 0.06$ $R^2 = 35\%$	$y = 0.59x - 0.14$ $R^2 = 40\%$	$y = 0.94x - 0.11$ $R^2 = 76\%$

[a] ac—atmospheric correction; the variables x and y refer to *in situ* Chla and satellite Chla respectively.

Table 2b. Log–log model II regression statistics for total absorption coefficient (a_{total}). (The variables x and y refer to *in situ* a_{total} and satellite a_{total} respectively.)

Area	n	Moore and Aiken	MODIS
Overall	78	$y = 0.66x - 0.20$ $R^2 = 64\%$	$y = 0.85x - 0.01$ $R^2 = 54\%$
NS	21	$y = 1.32x + 0.12$ $R^2 = 46\%$	$y = 1.70x + 0.31$ $R^2 = 21\%$
CS	24	$y = 0.45x + 0.55$ $R^2 = 59\%$	$y = 0.61x - 0.43$ $R^2 = 51\%$
WEC	33	$y = 0.75x + 0.02$ $R^2 = 29\%$	$y = 1.2x + 0.63$ $R^2 = 40\%$

443 nm, absorption coefficient of phytoplankton at 675 nm and estimates of normalized water-leaving radiance (nL_w) at 412, 443, 488–490, 551–555 and 667–670 nm were compared with those derived from the satellite algorithms described above. The 26 satellite match-ups are comprised of seven images in the North Sea, eight in the Celtic Sea and 11 at L4 in the WEC.

2.3.4. Statistical tests for algorithm performance comparison. *In situ* and satellite data are independent (no prediction) and are both subject to error. Model II linear regression was therefore used to assess algorithm accuracy, since it minimizes the areas between the data points and the best line of fit. Algorithm performance was estimated on log-transformed values of a_{total}, a_{phy}, a_{CDOM}, Chla and TSM using the root mean square (RMS). The slope and the intercept were obtained from the model II regression. The RMS for discrete samples was calculated as follows:

$$RMS = \sqrt{\frac{\sum (x_{obs,i} - x_{mod,i})^2}{n - 2}}$$

where $x_{mod,i}$ is the modelled value of the ith element, $x_{obs,i}$ is the observed (or *in situ* or measured) value of the ith element and n is the number of elements.

3. Results

Table 1 summarizes the range in bio-optical parameters for each campaign. Chla concentrations were highly variable compared to a_{CDOM} and a_{total}. The maximum Chla concentration was found during D-261, in the Celtic Sea (figure 1). Maximum TSM, a_{CDOM} and a_{phy} were found in the North Sea (Belgica 2002-14 cruise data) (figure 1). The WEC data (L4 Plymouth time series) showed the lowest a_{total} values. The East coast of the UK was characterized by highly turbid coastal waters (7–82 formazine turbidity units (FTU), mean 21 ± 12 FTU; personal communication, Alice Chapman, Environment Agency).

3.1. Chlorophyll-a concentration

Comparisons of satellite and *in situ* Chla concentrations are presented in figure 3. SeaWiFS OC4v4 using RSDAS ac, with the Bright Pixel implemented over high TSM waters, performed better than all other algorithms, and gave the best slope (1.14), the least scatter ($R^2 = 80\%$) and the lowest RMS (0.24; figure 3(a)). MODIS tended to show a higher scatter, especially at the lowest and highest Chla values (figures 3(c)–(e)). Of the three MODIS chlorophyll algorithms tested, chlor_a_3 gave the best Chla retrieval, followed by chlor_a_2 (table 2a; figure 3(e)), and chlor_MODIS gave the lowest estimate of Chla (table 2a; figure 3(c)). The absorption model was more accurate than chlor_a_2 and chlor_MODIS and gave the third best estimate of Chla concentrations (figure 3(b)), whereas the SeaWiFS OC4v4 with the standard NASA ac was not as accurate as SeaWiFS OC4v4 with RSDAS ac, especially for the North Sea (figure 3(f)).
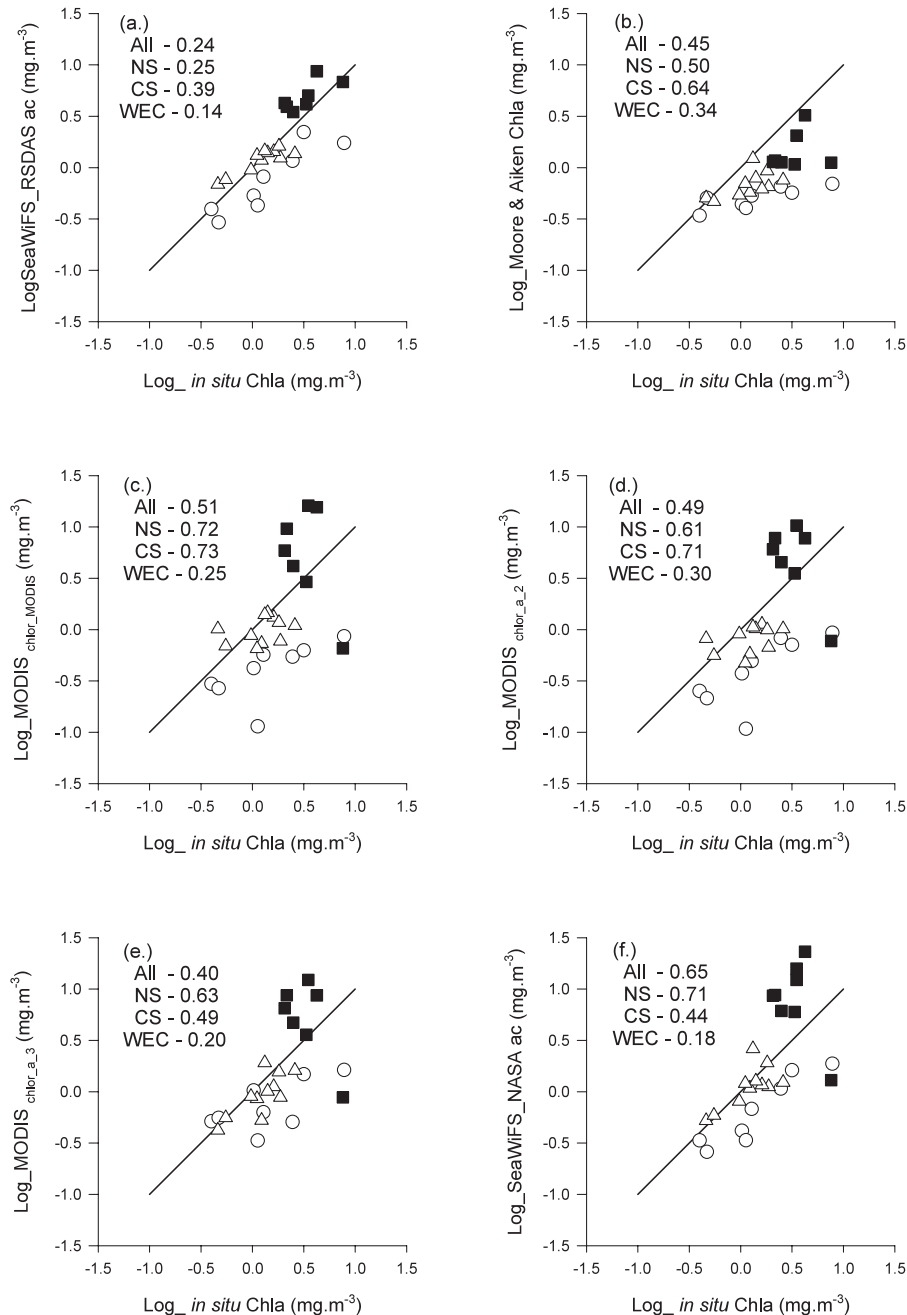
Figure 3. Scatter plots of log transformed *in situ* Chla and satellite derived Chla concentrations for (a) SeaWiFS OC4v4 with RSDAS atmospheric correction, (b) Moore and Aiken absorption model with RSDAS atmospheric correction, (c) chlor_MODIS, (d) chlor_a_2, (e) chlor_a_3 and (f) SeaWiFS OC4v4 with NASA atmospheric correction. The solid line represents a 1:1 relationship; O Celtic Sea (CS), △ Western English Channel (WEC) ■North Sea (NS). The RMS is given for each area.

On a regional basis, SeaWiFS OC4v4 with RSDAS ac gave the most accurate retrieval of Chla in all three study areas. The SeaWiFS NASA ac and MODIS algorithms consistently overestimated Chla in the North Sea, whereas the absorption model was more accurate. The absorption model however tended to underestimate Chla in all areas. SeaWiFS OC4v4 with NASA ac and MODIS chlor_a_3 were more accurate in the Celtic Sea and WEC. Chla maps for each model for the 12th June 2003 in the WEC and the Celtic Sea are illustrated in figure 4. From these images and figure 3 it is clear that the absorption model underestimated Chla, and that SeaWiFS

OC4v4 with NASA ac and all MODIS algorithms gave slightly higher Chla concentrations compared to SeaWiFS OC4v4 with RSDAS ac, especially in the Irish Sea and coastal areas of the WEC (figures 4(a) and (f)). Although chlor_a_3 showed some apparent striping features (figure 4(e)), this did not affect the estimates of Chla concentration because stations in the Celtic Sea and WEC were located on stripe-free pixels.

3.2. Inherent optical properties

3.2.1. Total absorption coefficient. Figures 5(a) and (b) compare *in situ* total absorption coefficients with those
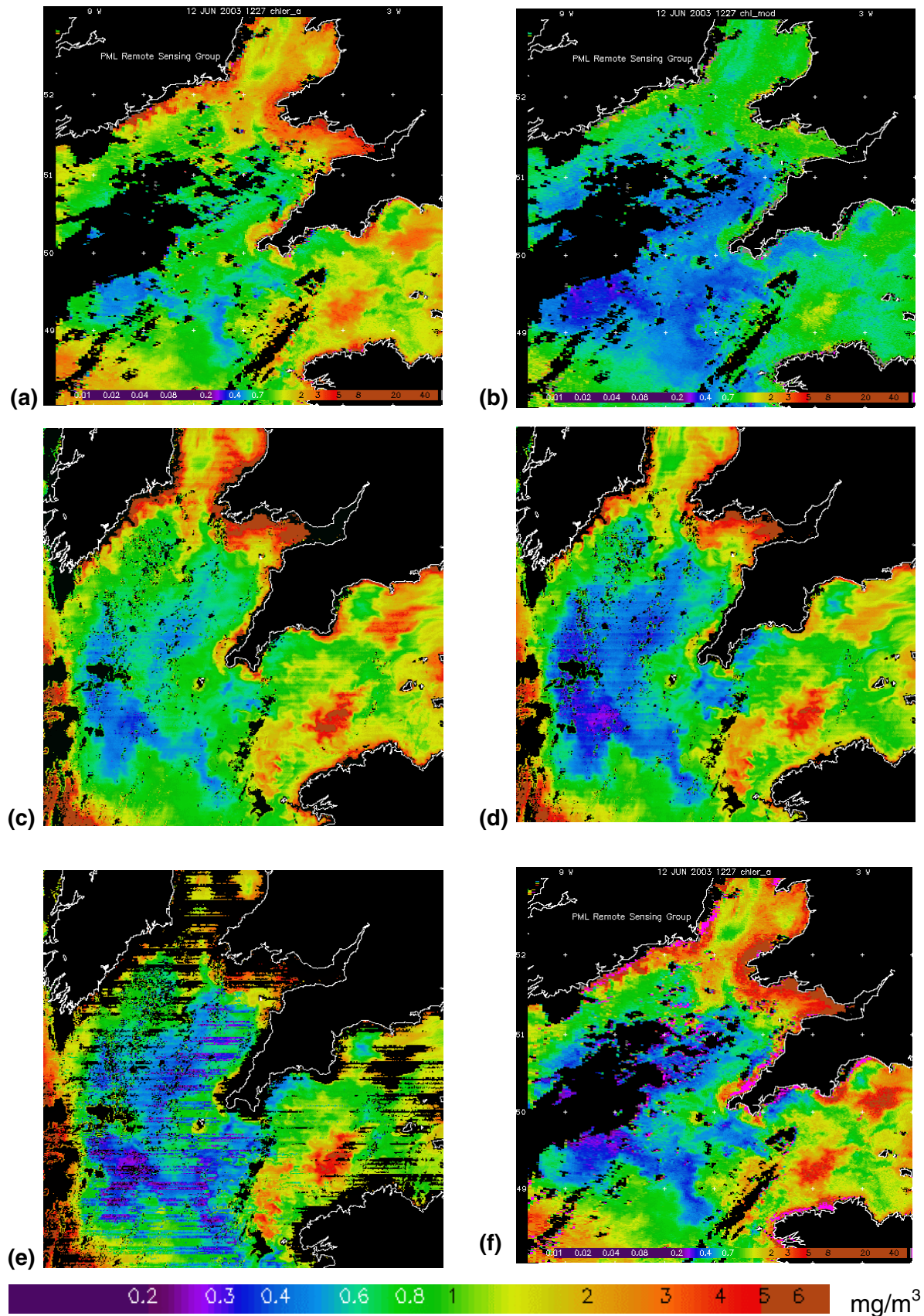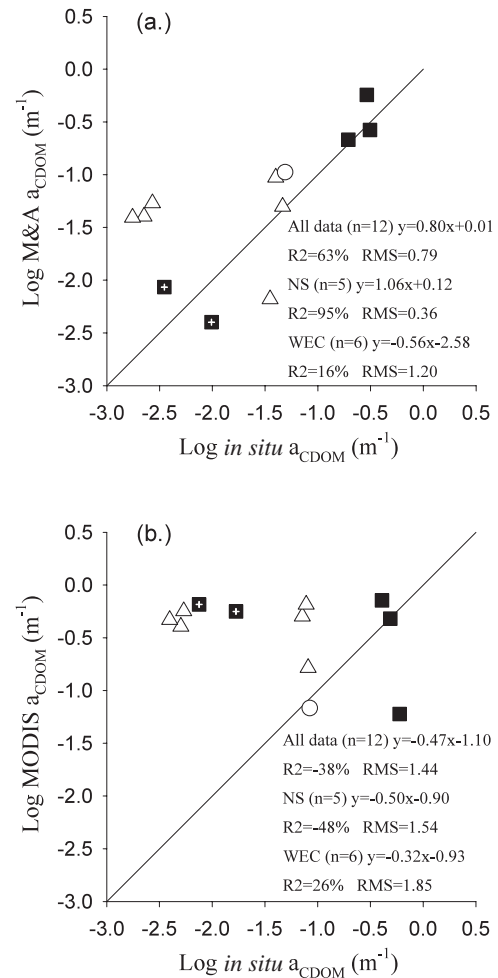
Figure 4. Comparison of chlorophyll concentrations for 12 June 2003 for the WEC, Irish and Celtic Seas from (a) SeaWiFS OC4v4 with RSDAS ac (12h27), (b) the Moore and Aiken absorption model with RSDAS ac (12h27), (c) chlor_MODIS (11h10), (d) chlor_a_2 (11h10), (e) chlor_a_3 (11h10) and (f) SeaWiFS OC4v4 with standard NASA ac (12h27). All images were scaled to the RSDAS colour scale (from 0.2 to 5 mg m^{-3} shown at the bottom of the figure).
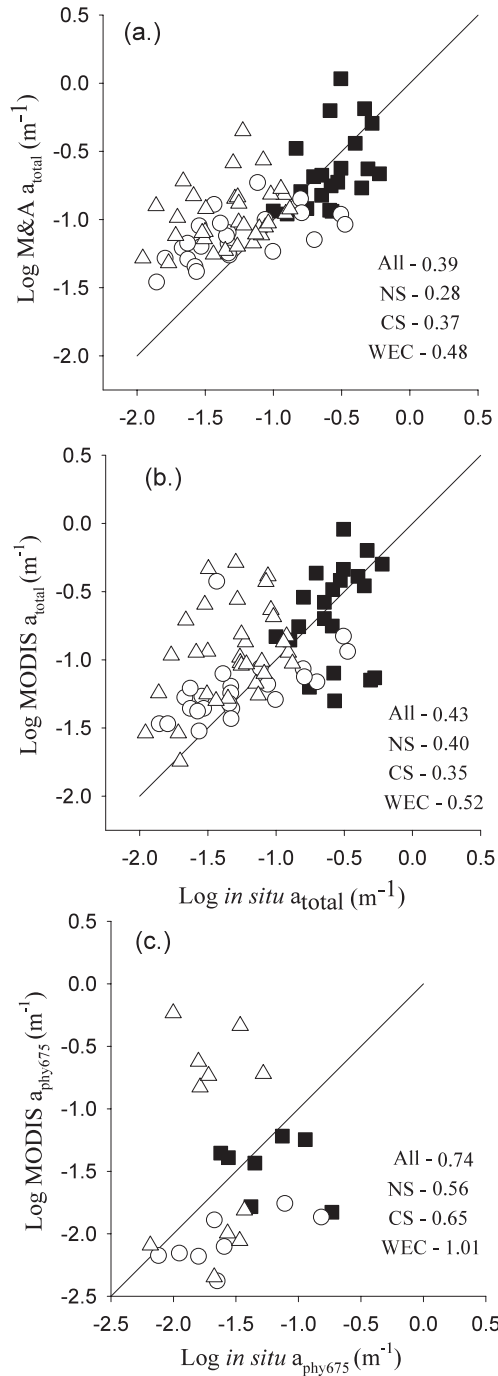
Figure 5. Scatter plots of log transformed *in situ* absorption coefficient and satellite algorithm derived absorption coefficient of $a_{total(412;443;488-490)}$: (a) Moore and Aiken absorption model, (b) MODIS and (c) $a_{phy(675)}$ for MODIS ($n = 26$). Symbols as per figure 3. The RMS is given for each area.

Figure 6. Scatter plots of log transformed *in situ* and satellite algorithm derived a_{CDOM} for (a) the Moore and Aiken absorption model and (b) MODIS. Symbols as per figure 3 except for ⊡ UK coast of NS, ■ Belgian coast of NS. Model II regression statistics and RMS are given for each area.

a higher intercept. The absorption model overestimated a_{total} at low *in situ* values ($0.03 < a_{total} < 0.06$ m^{-1}) in the Celtic Sea and the WEC (table 2b; figures 5(a), (b)); however, it still performed better than MODIS except for the East Coast of the UK where the retrieval accuracy was similar.
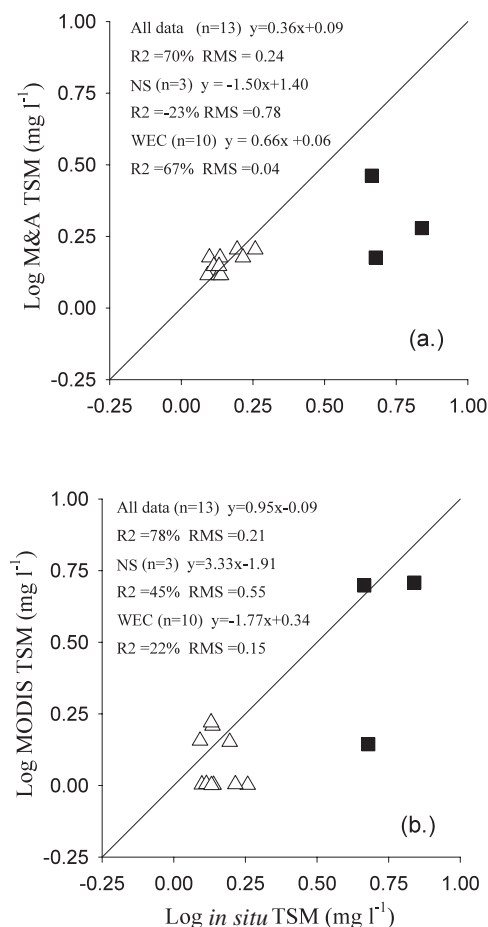
3.2.2. Phytoplankton absorption coefficient ($a_{phy(675 nm)}$). The retrieval of the phytoplankton absorption coefficient by MODIS (MOD-21, parameter 31) is given in figure 5(c). There was poor agreement between MODIS estimates and *in situ* values of $a_{phy(675)}$, especially for the WEC, where MODIS grossly overestimated absorption. The best retrieval was found in the North Sea.

3.2.3. CDOM absorption coefficient (a_{CDOM}). Only twelve match-ups were coincident with *in situ* CDOM data. Eleven were located in coastal, optically complex waters of the North Sea and WEC, and one in phytoplankton dominated waters, on the shelf of the Celtic Sea (table 1). The absorption model retrieves a_{CDOM} at 443 nm and MODIS retrieves a_{CDOM} at 400 nm (figure 6). Overall, the absorption model was more

derived from the absorption model (figure 5(a)) and MODIS (figure 5(b)) for the 26 match-ups at three wavelengths: 412 nm (MOD-36, parameter 32), 443 nm (MOD-36, parameter 33) and 488–490 nm (MOD-36, parameter 34). Both the absorption model and the MODIS algorithm overestimated a_{total} at low *in situ* a_{total} values (figures 5(a) and (b)). Overall, the absorption model showed better a_{total} retrieval compared to MODIS (table 2b and figures 5(a) and (b)), which resulted in
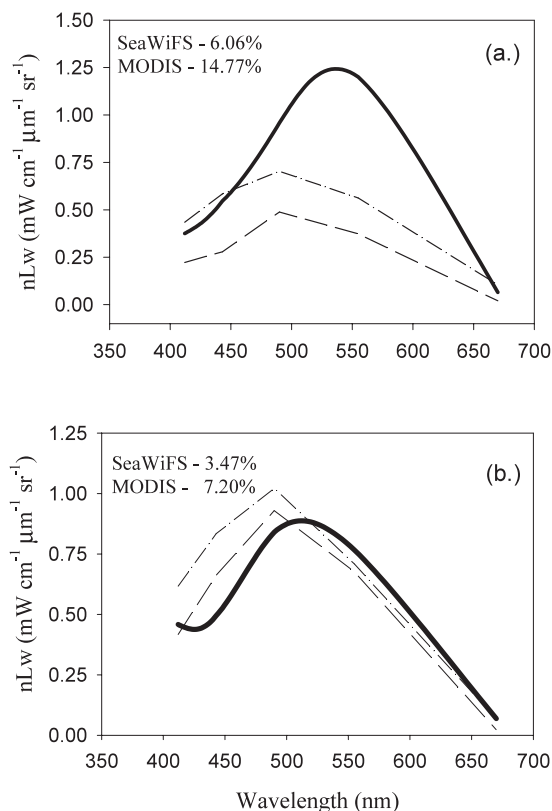
Figure 7. Scatter plots of log transformed *in situ* TSM and satellite algorithm derived TSM for (a) the Moore and Aiken absorption model and (b) MODIS. Symbols as per figure 3. Model II regression statistics and RMS are given for each area.

Figure 8. *In situ* nL_w and satellite derived nL_w for SeaWiFS and MODIS at L4 station (WEC) on (a) 19 May 2003 and (b) 20 June 2003. —— *in situ* nL_w, — · — SeaWiFS nL_w, – – – MODIS nL_w. The averaged percentage difference between *in situ* and satellite nL_ws is given for each match-up.

accurate, with a higher percentage variance explained and a lower RMS compared to MODIS. On a regional basis, the absorption model performed better in all regions, whereas MODIS overestimated CDOM along the East coast of the UK and in the WEC.

3.2.4. Total suspended material (TSM). Total suspended material was only sampled on cruise Belgica 2002-14, in the North Sea, and in the WEC, at L4 (table 1; figure 1). Generally, MODIS was more accurate than the absorption model, which consistently underestimated TSM concentrations in the North Sea (figure 7), although the latter performed better in the WEC at lower concentrations of TSM (table 1).

3.2.5. Normalized water-leaving radiance (nL$_w$). In *situ* nL_w measurements in the WEC for the 19th May and 20th June 2003 were the only two good quality match-ups for the entire data set. Based on these, SeaWiFS was more accurate at estimating nL_w than MODIS and SeaWiFS consistently had higher nL_ws than MODIS (figure 8). SeaWiFS nL_w was accurate at 412 nm (4% difference), but was less accurate at 667–670 and 551–555 nm (up to 6% difference). MODIS gave systematically higher percentage differences, which were 1.4–4.7 times greater than SeaWiFS. The best agreement between

MODIS and *in situ* nL_ws was at 412 nm (5% difference), but it was significantly less accurate at 551–555 (9% difference) and 667–670 nm (27% difference).

4. Discussion

The objective of this paper is to evaluate the performance of different satellite sensors and algorithms in estimating bio-physical products, particularly in optically complex coastal waters. We were also able to compare differences in radiometry between the sensors using a limited number of nL_w observations for SeaWiFS and MODIS. We tested the effect of atmospheric correction on SeaWiFS estimates of chlorophyll concentration using NASA ac and RSDAS ac with the Bright Pixel for turbid waters. SeaWiFS OC4v4 with RSDAS ac and the absorption model use the same radiances, which enabled us to assess the performance of an empirical band ratio Chla algorithm and a fully analytical IOP model, independent of other effects. Comparison of the three MODIS algorithms also enabled us to evaluate empirical and semi-analytical algorithms which use different band ratios but the same sensor radiometry.

4.1. Atmospheric correction and normalized water-leaving radiance

Atmospheric correction is critical for the accurate estimation of nL_w. SeaWiFS and MODIS NASA standard products

883

use 'virtually' the same ac (Siegel *et al* 2000, Vermote and Vermeulen 1999) but its performance can differ slightly due to differences in band centres in the visible and NIR and aerosol model libraries. SeaWiFS uses the 765 nm band, which is designed to monitor oxygen absorption, but this can reduce the radiance by 10–15% (Carder *et al* 2002). To avoid this, MODIS uses a band centred at 748 nm, which should lead to a more accurate ac and therefore nL_w. Darecki and Stramski (2004) found that the current MODIS ac failed to retrieve upwelling radiance in the Baltic. In coastal turbid waters, high concentrations of TSM lead to significant backscatter, resulting in reflectance at near-infrared wavelengths. These waters are termed 'Bright Pixel' waters and require specific ac procedures (Moore *et al* 1999). In these waters the conventional ac used for MODIS and SeaWiFS fails (Andre and Morel 1991, Gordon and Wang 1994), because it assumes that water-leaving radiance in the near-infrared is zero (Ruddick *et al* 2000, Siegel *et al* 2000). Moore *et al* (1999) proposed a coupled hydrological atmospheric model for turbid waters which solves the water-leaving radiance and atmospheric path radiance in the near-infrared and showed that it has superior performance over the standard single-scattering approach. We processed SeaWiFS images using the Bright Pixel ac for waters flagged as turbid coastal waters ($\rho_w(670) > 0.003$), and the NASA ac for phytoplankton dominated waters (table 1). For the two match-ups in the WEC, SeaWiFS gave more accurate nL_w retrieval which suggests more accurate radiometry for SeaWiFs than MODIS. In the North Sea the RSDAS Bright Pixel ac was triggered and SeaWiFS with this ac consistently performed better than MODIS. Further work is required to test and improve the ac over optically complex waters for MODIS.

The quality of the atmospheric correction affects the quality of the nL_w, which is key to the estimation of the biophysical products, and any errors in nL_w will propagate to the other products. The radiometric objective of the NASA SeaWiFS mission is to estimate nL_w to within ±5%. For the limited number of match-ups we had, satellite derived nL_w showed poor agreement with *in situ* values which could be associated with the atmospheric correction used. For wave bands 412 to 488–490 nm, the WEC data suggests that this was probably achieved for SeaWiFS but not for MODIS. SeaWiFS bands 412 and 490 were the most accurate and band 555 was less accurate, but this did not adversely affect the R_{rs} ratios since SeaWiFS Chla retrieval was the most accurate of the two sensors. NASA also expects the same radiometric performance for MODIS. Based on these two match-ups in the WEC, we found that the nL_w retrieval accuracy of MODIS was between 6 and 28% (figure 8).

4.2. Chlorophyll-a

The regions sampled spanned a limited range of Chla concentrations (0.4–7.8 mg m^{-3}) which are well within the calibration range of each of the algorithms analysed. The environments tested were variable and included optically complex waters with medium TSM and CDOM concentrations on the Belgian coast, high TSM and low CDOM on the South Eastern UK coast of the North Sea, and phytoplankton dominated waters in the Celtic Sea (table 1). Babin *et al* (2003) found similar proportions of TSM and CDOM for the North Sea and WEC.

Theoretically SeaWiFS OC4v4 with NASA ac should be accurate in the Celtic Sea and less accurate in the North Sea and WEC. As may be expected, SeaWiFS with NASA ac and RSDAS ac showed the best Chla retrieval in the Celtic Sea and SeaWiFS with RSDAS ac showed accurate Chla retrieval in all areas, including the optically complex coastal regions of North Sea and WEC. This could be partly explained by the fact that BP ac over turbid waters leads to more accurate nL_w and that the more optically complex environments studied did not have very high CDOM concentrations. In the Baltic Sea, where CDOM concentrations are exceptionally high, Darecki and Stramski (2004) found that SeaWiFS significantly underestimated Chla. Based on the limited observations in the WEC, we found that SeaWiFS retrieved nL_w better than MODIS, which is attributable to both better radiometric accuracy and ac. This may explain why SeaWiFS gave more accurate Chla concentrations in highly turbid environments, such as the UK and Belgian coasts. For a single image on 12 June 2003, all ocean colour algorithms, except the absorption model, predicted relatively high Chla concentrations in the Celtic Sea and WEC, especially on the Southern Irish and Welsh coasts and in the WEC north of Brittany (figure 4). There were, however, subtle differences in the Chla concentration given by SeaWiFS OC4v4 with RSDAS ac and SeaWiFS OC4v4 with NASA ac and MODIS algorithms. The SeaWiFS OC4v4 with NASA ac overestimated Chla concentrations near the coast and this algorithm and MODIS chlor_a_3 underestimated Chla off the western approach, compared to SeaWiFS OC4v4 with RSDAS ac.

Gordon *et al* (1983b) suggested that the pigment concentration can be derived from the radiance ratio with an error of ±20%. In this study, we found a difference of 44% between SeaWiFS RSDAS ac and *in situ* Chla, and for MODIS chlorophyll algorithms between 78 and 88%. Both SeaWiFS OC4v4 and all MODIS chlorophyll algorithms tended to overestimate Chla in the North Sea probably due to the influence of CDOM, albeit low, and also to the higher Chla concentrations encountered. MODIS chlor_a_2, the SeaWiFS analogue, showed some of the lowest estimates, except in the North Sea. MODIS chlor_a_2 and SeaWiFS OC4v4 use mainly longer wavelengths than 443 (i.e. 488:551; 490:555 or 510:555 band ratios) and these algorithms tend therefore to be less affected by the higher CDOM absorption in the North Sea (table 1), which results in a more accurate estimate of chlorophyll. By comparison, Darecki and Stramski (2004) found that the systematic error in the Baltic Sea was higher for chlor_a_3 than for chlor_a_2.

To assess the effect of differences in algorithm type, we used the radiances from each sensor to re-calculate Chla using SeaWiFS Oc4v4 and MODIS chlor_a_2 algorithms (figure 9). The solid and dashed curves in figure 9 are the power law regressions for MODIS and SeaWiFS based on the maximum R_{rs} ratios which correspond to the data extracted from the satellite image match-ups. Re-calculated Chla concentrations using SeaWiFS OC4-v4 and SeaWiFS radiances were higher compared to those re-calculated with MODIS radiances. This was due to the higher radiances from SeaWiFS. For chlor_a_2 the effect of using different radiance inputs on the predicted Chla was less apparent, suggesting that this empirical algorithm is less sensitive to differences in radiance compared to OC4v4. All scatter
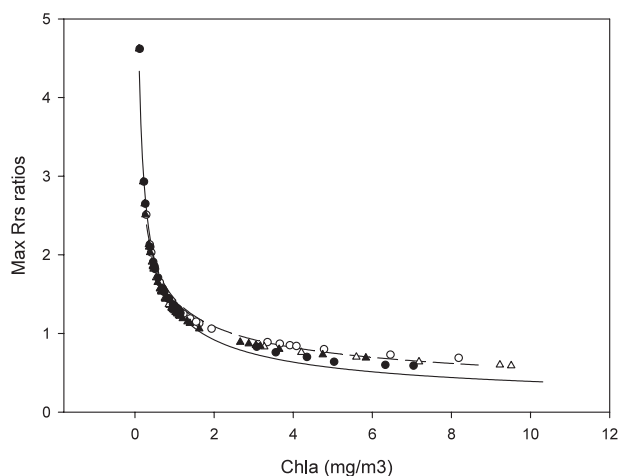
Figure 9. Scatter plot of maximum R_{rs} band ratios versus Chla, extracted from processed satellite images and estimated from modelled SeaWiFS OC4v4 and modelled MODIS chlor_a_2. ——— power law for MODIS max R_{rs} ratios, – – – power law for SeaWiFS max R_{rs} ratios, ○ modelled OC4v4 Chl-a using SeaWiFS R_{rs}, ● modelled OC4v4 Chl-a using MODIS R_{rs}, △ modelled chl_a_2 using MODIS R_{rs}, ▲ modelled chl_a_2 using SeaWiFS R_{rs}.

plots were closer to the power law regression based on the maximum R_{rs} of SeaWiFS compared to MODIS, suggesting an improvement in the radiometric accuracy of MODIS is necessary. This may be achieved using a different atmospheric correction.

The MODIS band ratio chlor_MODIS gave the least accurate Chla concentrations, due to the poorer radiometric accuracy of MODIS. This algorithm is also simplistic and always uses the 443 and 551 bands which compounds the spectral influence of CDOM, especially in the North Sea. Of the MODIS algorithms tested, chlor_a_3 exhibited the best performance which is probably due to the fact that this algorithm corrects for phytoplankton pigment packaging effects and CDOM (Carder *et al* 2002). Darecki and Stramski (2004) found that out of 707 Chla estimates of chlor_MODIS and chlor_a_3, 35 were ten times higher than *in situ* values. In our study, SeaWiFS with RSDAS ac, however, always gave more accurate estimates of Chla, even at the highest CDOM concentrations, which suggests that improvements in MODIS ac is necessary before SeaWiFS is non-operational. Although MODIS could be recalibrated, some of the inherent differences between SeaWiFS and MODIS cannot be corrected due to differences in sensor characteristics.

Since the oceans are optically dark bodies the signal–noise ratio (SNR) is also important in the accuracy to which nL_w and consequently Chla can be determined. MODIS has a higher SNR (Esaias *et al* 1998) and should be capable of spanning the nominal range of Chla from 0.01 to 20 mg m^{-3} better than SeaWiFS; however, our data showed that this was not the case. There is a fundamental design difference between the two sensors. For SeaWiFS, the observation angle can be tilted away from the sun, which reduces sun glint, but for MODIS the observation angle is fixed and large areas of the swath may be covered by sun glint (Barnes *et al* 1998). Pixels with high sun glint will have been eliminated by using the MODIS flags for nL_w, but since we used some questionable flags for Chla there

may be some other contamination effects. Also, the Terra-MODIS instrument experienced several technical problems (e.g. detector striping, mirror alignment, power shutdown), leading to some data loss since the instrument went into standby mode. The instable calibration of MODIS and excess radiances due to stray light effects may affect the accuracy of Terra-MODIS radiometry and therefore the quality of nL_w estimates from which the other products are derived.

Using data from the Atlantic and WEC, Moore and Aiken (2004) found that their bio-optical model explained a higher percentage of variance and had a lower RMS than SeaWiFS OC4v4. We found that SeaWiFS OC4v4 performed better even though the radiance and ac were the same for each algorithm. The absorption model gave the third best estimate of Chla. It derives Chla concentration from $a_{total}(443)$, corrected for CDOM absorption, and it is not affected by TSM, since the algorithm is independent of particle backscatter. It accurately estimated the IOPs (figures 5 and 6 and see below), which suggests that further improvement in the iteration to Chla or better parametrization of a_{phy} is necessary, especially in the Celtic Sea and WEC.

Some authors have suggested that differences in *in situ* protocols may adversely affect the calibration and performance of satellite algorithms (e.g. Balch *et al* 1989). The SeaWiFS chlorophyll algorithm was calibrated using the SeaBASS data set comprising 750 cruises and a wide range of Chla HPLC protocols. The absorption model was calibrated with data using the same Chla HPLC protocol, but the accuracy of SeaWiFS Chla retrieval was always better with the RSDAS ac. Although the size of the calibration dataset will contribute to differences in performance, it would seem for this study that variations in *in situ* protocols have a negligible effect on algorithm performance.

Other authors have suggested that differences in sampling time and satellite overpass or error in ship and satellite collocation can significantly bias the validation exercise (Balch *et al* 1989, Doerffer and Fischer 1994). This is especially important in regions where tidal currents determine the concentration of near-surface suspended material (Doerffer *et al* 1989) such as the South coast of the UK. In this study, SeaWiFS always had a greater time difference between overpass and *in situ* sampling than MODIS which suggests that differences in sampling time did not have a significant effect on satellite validation.

4.3. Inherent optical properties

The absorption model consistently gave more accurate estimates of a_{total} and a_{CDOM}, although MODIS did show a similar accuracy for a_{total} along the South East coast of the UK, which has the highest variability in IOPs (Hill *et al* 1993, Brown *et al* 1999). MODIS yielded more accurate estimates of TSM in the turbid North Sea, albeit for few data, but not in the WEC. The reason for this difference may be due to both the parametrization of the models and the fact that the absorption model uses BP ac over turbid waters, but also the type of sediments and particle size distribution (Mikkelsen 2002). The absorption model is fully analytical and solves TSM from backscatter, whereas the TSM MODIS algorithm is based directly on reflectance band 551

and is therefore sensitive to errors in estimates of marine reflectance.

MODIS retrieval of $a_{\mathrm{phy(675)}}$ showed high scatter, especially in the WEC where MODIS also overestimated a_{total} and a_{CDOM}. If $a_{\mathrm{phy(675)}}$ is within a predetermined Chla range, chlor_a_3 is calculated from an empirical relationship between $a_{\mathrm{phy(675)}}$ and Chla. If $a_{\mathrm{phy(675)}}$ is outside that range, Chla is calculated from the R_{rs} ratio 488:551. *In situ* $a_{\mathrm{phy(675)}}$ exhibits high regional variability in both phytoplankton dominated (Lutz *et al* 1996) and CDOM-TSM dominated regions, where the presence of high TSM can cause a flattening in the 675 nm absorption peak (Sathyendranath *et al* 1987). A more accurate estimation of $a_{\mathrm{phy(675)}}$ in the presence of TSM based on prior knowledge of regional variability may improve the performance of MODIS chlor_a_3, although this has proven difficult in the Baltic Sea (Darecki and Stramski 2004). The parametrization of $a_{\mathrm{phy(675)}}$ does not seem to be as accurate as simply applying the BP ac for optically complex waters. For the improvement of estimates of bio-physical products in turbid waters, future work should focus on testing this and other bio-optical models with MODIS radiances and the BP ac.

MODIS tended to overestimate a_{CDOM} in the North Sea and WEC, and this poor retrieval may be attributed partly to striping, which was frequently seen on many of the CDOM images and is a common feature of MODIS due to the fixed camera alignment. The Moore and Aiken model gave the best a_{CDOM} retrieval, especially for the North Sea Belgian coast where there was the highest CDOM signal. CDOM concentrations in the other regions were typical of phytoplankton dominated waters (Kirk 1994) and both algorithms overpredicted a_{CDOM} in these regions, which resulted in a disparate partitioning between a_{CDOM} and a_{phy} and thus lower Chla values (figures 1 and 3). CDOM concentrations for the South East coast of the UK were also low, and MODIS tended to overestimate CDOM in this area. MODIS chlor_a_2 does not correct for CDOM, which may explain why this algorithm gave more accurate Chla concentrations on the North Sea UK coast.

5. Conclusions

SeaWiFS with RSDAS ac gave the best estimates of Chla concentration in the phytoplankton dominated waters of the Celtic Sea and in the more optically complex waters of the WEC and North Sea. This was mainly attributed to a better radiometric accuracy due to the implementation of the Bright Pixel ac over turbid waters and the sensor geometry.

MODIS algorithms were not as accurate as SeaWiFS OC4v4 with RSDAS ac, which may be attributed to radiometry and poorer atmospheric correction over turbid waters which resulted in lower estimates of nL_{w}. Of the MODIS algorithms tested, chlor_a_3, which corrects for CDOM and phytoplankton pigment packaging, was the most accurate and chlor_MODIS was the least accurate. Compared to the fully analytical absorption model of Moore and Aiken (2004), MODIS consistently overestimated a_{total} and a_{CDOM} and the absorption model gave the best retrieval of IOPs in all environments but was less accurate at predicting Chla. An improvement in the iteration procedure of the absorption model (Moore and Aiken 2004) in converting $a_{\mathrm{phy(443)}}$ to Chla is required to give more accurate estimates of Chla in these optically complex environments.

Appendix A. Glossary

ATBD	Algorithm theoretical basis document
BP ac	Bright Pixel atmospheric correction
Chla	Chlorophyll-a concentration (mg m^{-3})
CDOM	Coloured dissolved organic matter (m^{-1})
CZCS	Coastal zone colour scanner
DAAC	Distributed Active Archive Centre
GAC	Global area coverage
HRPT	High resolution picture transmission
IOPs	Inherent optical properties
LAC	Local area coverage
MODIS	Moderate-resolution imaging spectroradiometer
NASA ac	NASA atmospheric correction
NIR	Near-infrared
OD	Optical density (relative absorbance units)
RSDAS ac	Remote Sensing Data Analysis Service (PML) atmospheric correction
SeaWiFS	Sea-viewing wide field-of-view sensor
TSM	Total suspended matter (mg l^{-1})
WEC	Western English Channel
$a(\lambda)$	Absorption coefficient (m^{-1})
$b_{\mathrm{b}}(\lambda)$	Backscattering coefficient (m^{-1})
$\varepsilon_{\mathrm{a}}(\lambda)$	Ratio of a_{490} to a_{510}
$\varepsilon_{\mathrm{bb}}(\lambda)$	Ratio of $b_{\mathrm{b}490}$ to $b_{\mathrm{b}510}$
$f_0(\lambda)$	Mean extraterrestrial solar irradiance (mW cm^{-2} μm^{-1})
$L_{\mathrm{w}}(\lambda)$	Water-leaving radiance (mW cm^{-2} μm^{-1} sr^{-1})
$nL_{\mathrm{w}}(\lambda)$	Normalized water-leaving radiance (mW cm^{-2} μm^{-1} sr^{-1})
Q	The Q-factor, ratio of upwelling radiance to radiance
$R_{\mathrm{rs}}(\lambda)$	Remote-sensing reflectance (sr^{-1})
$\rho_{\mathrm{w}}(\lambda)$	Above-water reflectance (dimensionless)

Appendix B. Description of algorithms and models

Algorithm	General form
SeaWiFS OC4-v4 (O'Reilly *et al* 1998, 2000)	$[\text{Chl-a}] = 10^{(a+bR+cR^2+dR^3+eR^4)}$ R is the $\log_{10}$ of the maximum band ratio: $R = \log_{10}\{\max[R_{\text{rs}}(443)/R_{\text{rs}}(555), R_{\text{rs}}(490)/R_{\text{rs}}(555), R_{\text{rs}}(510)/R_{\text{rs}}(555)]\}$ and the coefficients are determined by linear regression $a = 0.366$; $b = -3.067$; $c = 1.930$; $d = 0.649$; $e = -1.532$
Terra-MODIS chlor_MODIS (MOD-19, parameter 14) Chlorophyll-a concentration for case 1 waters (Clark *et al* 1997)	$\log_{10}[\text{Chl-a}] = a\left[\log\left(\frac{R_{\text{rs}}(443)}{R_{\text{r}}(551)}\right)^3\right] + b\left[\log\left(\frac{R_{\text{rs}}(443)}{R_{\text{r}}(551)}\right)^2\right] + c\left[\log\left(\frac{R_{\text{rs}}(443)}{R_{\text{r}}(551)}\right)\right] + d$ The coefficients are: $a = -1.594$; $b = 1.122$; $c = -1.396$; $d = -0.0922$
Terra-MODIS chlor_a_2 (MOD-21, parameter 26) Chlorophyll-a concentration for case 2 waters (Carder *et al* 1999b)	$\log_{10}[\text{Chl-a}] = 0.283 - 2.753R + 1.457R^2 + 0.659R^3 - 1.403R^4$ R is the $\log_{10}$ of the maximum band ratio: $R = \log_{10}[\max[R_{\text{rs}}(443)/R_{\text{rs}}(551), R_{\text{rs}}(488)/R_{\text{rs}}(551)]]$
Terra-MODIS chlor_a_3 (MOD-21, parameter 27) Chlorophyll-a concentration for case 2 waters (Carder *et al* 1999a)	For default cases, the chlorophyll-a concentration was calculated from emprirical algorithms: $\text{chlor\_a\_3} = 10^{(0.289-3.20R+1.2R^2)}$ where $R = \log_{10}\frac{R_{\text{rs}}(488)}{R_{\text{rs}}(551)}$
Terra-MODIS CDOM absorption coefficient. (MOD-21, parameter 30) (Carder *et al* 1999a)	$a_{\text{ys}}(400)_{\text{emp}} = 1.5 \times \left(10^{-1.147-1.963\rho_{15}-1.01\rho_{15}^2+0.856\rho_{25}+1.702\rho_{25}^2}\right)$ where ρ_{ij} are log of the ratio of the remote sensing reflectance of MODIS channel i to channel j
Terra-MODIS Phytoplankton absorption coefficient (MOD-21, parameter 31) (Carder *et al* 1999a)	Derived from the $a_{\text{CDOM}(400)}$ and $a_{\text{phy}(675)}$: $a_{\text{phy}}(400)_{\text{emp}} = 0.328 \times \left(10^{-0.919+1.037\rho_{25}-0.407\rho_{25}^2-3.531\rho_{35}+1.702\rho_{35}^2-0.008}\right)$
PML Bio-optical model (Moore and Aiken 2004) IOP$_1$ (absorption)	$a(\lambda_j) = \dfrac{\mathfrak{R}_j F_j \left[\varepsilon_{\text{bb}}b_{\text{bw}}(j) - b_{\text{bw}}(i) + \chi a_{\text{w}}(i)\rho_{\text{w}}(i) - a_{\text{w}}(j)\varepsilon_{\text{bb}}\rho_{\text{w}}(j)\right]}{\varepsilon_{\text{bb}}\rho_{\text{w}}(i) - \chi\varepsilon_{\text{a}}\rho_{\text{w}}(i)}$ $\mathfrak{R}$ is the interface term, ε is the slope, ρ, the reflectance and i and j are two sensors bands with $\lambda_i < \lambda_j$ (for instance, $\lambda_i = 490$ nm and $\lambda_i = 510$ nm)
PML bio-optical model (Moore and Aiken 2004) IOP$_2$ (backscattering)	$b_{\text{b}}(\lambda_j) = \dfrac{\chi\varepsilon_{\text{a}}b_{\text{bw}}(j)\rho_{\text{w}}(i) - b_{\text{bw}}(i)\rho_{\text{w}}(j) + \left[\dfrac{\rho_{\text{w}}(i)\rho_{\text{w}}(j)}{\mathfrak{R}_i F_i}\right] \times [a_{\text{w}}(i) - \varepsilon_{\text{a}}a_{\text{w}}(j)]}{\varepsilon_{\text{bb}}\rho_{\text{w}}(i) - \chi\varepsilon_{\text{a}}\rho_{\text{w}}(i)}$

References

Andre J M and Morel A 1991 Atmospheric correction and interpretation of marine radiances in CZCS imagery, revisited *Oceanol. Acta* **14** 3–22

Babin M, Stramski D, Ferrari G M, Claustre H, Bricaud A, Obolensky G and Hoepffner N 2003 Variations in the light absorption coefficients of phytoplancton, non algal particles and dissolved organic matter in coastal waters around Europe *J. Geophys. Res.* **108** 3211 (doi: 10.1029/2001JC000882)

Balch W M, Abbott M R and Eppley R W 1989 Remote sensing of primary production: a comparison of empirical and semi-analytical algorithms *Deep-Sea Res.* **36** 281–95

Barlow R G, Cummings D G and Gibb S W 1997 Improved resolution of mono- and divinyl chlorophylls a and b and zeaxanthin and lutein in phytoplankton extracts using reverse phase C-8 HPLC *Mar. Ecol. Prog. Ser.* **161** 303–7

Barnes W L, Thomas S P and Salomonson V V 1998 Prelaunch characteristics of the moderate resolution imaging spectroradiometer (MODIS) on EOS-AM1 *IEEE Trans. Geosci. Remote Sens.* **36** 1088–99

Brown J, Hill A E, Fernand L and Horsburgh K J 1999 Observations of a seasonal jet-like circulation at the central North Sea cold pool margin *Estuarine Coastal Shelf Sci.* **44** 343–55

Carder K L, Chen F R, Lee Z P, Hawes S and Kamykowski D 1999a Semi-analytic MODIS algorithms for chlorophyll a and absorption with bio-optical domains based on nitrate-depletion temperatures *J. Geophys. Res.* **104** 5403–21

Carder K L, Chen F R, Lee Z, Hawes S K and Cannizzaro J P 1999b Case 2 chlorophyll a *MODIS ATBD-19* University of South Florida, USA

Carder K, Liu Q and Carter C 2002 Atmospheric correction over ocean for production of remote sensing reflectance v.5 *MODIS ATBD* University of South Florida, USA

Clark D K, Gordon H R, Voss K J, Ge Y, Broenkow W and Trees C 1997 Validation of atmospheric correction over the oceans *J. Geophys. Res.* **102** 17209–17

Darecki M and Stramski D 2004 An evaluation of MODIS and SeaWiFS bio-optical algorithms in the Baltic Sea *Remote Sens. Environ.* **89** 326–50

Doerffer R and Fischer J 1994 Concentrations of chlorophyll, suspended matter, and gelbstoff in Case II waters derived from satellite coastal zone color scanner data with inverse modeling methods *J. Geophys. Res.* **99** 7457–66

Doerffer R, Fischer J, Stossel M, Brockmann C and Grassl H 1989 Analysis of thematic mapper data for studying the suspended matter distribution in the coastal area of the german bight (North Sea) *Remote Sens. Environ.* **28** 61–73

Esaias W E *et al* 1998 An overview of MODIS capabilities for ocean science observations *IEEE Trans. Geosci. Remote Sens.* **36** 1250–65

Ferrari G M, Dowell M D, Grossi S and Targa C 1996 CDOM absorption, fluorescence and DOC relationships in the southern Baltic Sea. Evaluation of seasonal aspects *Mar. Chem.* **55** 299–316

Fu G, Baith K S and McClain C R 1998 SeaDAS: the SeaWiFS data analysis system *Proc. Conf. on 4th Pacific Ocean Remote Sensing (Qingdao, China)* pp 73–9

Gons H J 1999 Optical teledetection of chlorophyll-a in turbid inland waters *Environ. Sci. Technol.* **33** 1127–32

Gordon H R, Clark D K, Brown J W, Brown O B, Evans R H and Broenkow W W 1983b Phytoplankton pigment concentrations in the middle Atlantic bight comparison between ship determinations and coastal zone color scanner estimates *Appl. Opt.* **22** 30–6

Gordon H R and Morel A 1983 Remote assessment of ocean color for interpretation of satellite visible imagery: a review *Lecture Notes on Coastal and Estuarine Studies* vol 4, ed M Bowman (New York: Springer)

Gordon H R and Wang M 1994 Influence of oceanic whitecaps on atmospheric correction of SeaWiFS *Appl. Opt.* **33** 7754–63

Hill A E *et al* 1993 Dynamics of tidal mixing fronts in the North Sea *Phil. Trans. R. Soc.* **343** 431–46

Hooker S B, McCjain C R and Holmes A 1993 Ocean color imaging: CZCS to SeaWiFS *Mar. Technol. Soc. J.* **27** 3–15

Kirk J T O 1994 *Light and Photosynthesis in Aquatic Ecosystems* 2nd edn (New York: Cambridge University Press)

Lancelot C, Billen G, Sournia A, Weisse T, Colijn F, Veldhuis M J W, Davies A and Wassman P 1987 Phaeocystis blooms and nutrient enrichment in the continental coastal zones of the North Sea *Ambio* **16** 38–46

Lavender S J and Groom S B 1999 The SeaWiFS automatic data processing system (SeaAPS) *Int. J. Remote Sens.* **20** 1051–6

Lutz V A, Sathyendranath S and Head E J H 1996 Absorption coefficient of phytoplankton: regional variations in the North Atlantic *Mar. Ecol. Prog. Ser.* **135** 197–213

Mantoura R F C and Llewellyn C A 1983 The rapid determination of algal chlorophyll and carotenoid pigments and their breakdown products in natural waters by reverse- phase-high performance liquid chromatography *Anal. Chim. Acta* **152** 297–314

Mikkelsen O A 2002 Variation in the projected surface area of suspended particles: implications for remote sensing assessment of TSM *Remote Sens. Environ.* **79** 23–9

Mitchell G *et al* 2000 Determination of spectral absorption coefficients of particles, dissolved material, and phytoplankton for discrete water samples *Ocean Optics Protocols for Satellite Ocean Color Sensor Validation* revision 2 *NASA/TM 2000-209966* ed G S Fargion and J L Mueller (Greenbelt, MD: NASA Goddard Space Flight Center) pp 125–53

Moore G F and Aiken J 2004 A bio-optical model for the determination of inherent optical properties from reflectance data: applications to remotely sensed data from case 1 and case 2 waters *Appl. Opt.* submitted

Moore G F, Aiken J and Lavender S J 1999 The atmospheric correction of water colour and the quantitative retrieval of suspended particulate matter in case 2 waters: application to MERIS *Int. J. Remote Sens.* **20** 1713–33

Morel A and Prieur L 1977 Analysis of variations in ocean color *Limnol. Oceanogr.* **22** 709–22

Mueller J L and Austin R W 1995 *Ocean Optics Protocols for SeaWiFS Validation* revision 1 *NASA Tech. Memo. 104566(25)* ed S B Hooker, E R Firestone and J G Acker (Greenbelt, MD: NASA Goddard Space Flight Center)

Mueller J, Davis C, Arnone R, Frouin R, Carder K, Lee Z P, Steward R G, Hooker S, Mobley C D and McLean S 2000 Above-water radiance and remote sensing reflectance measurements and analysis protocols *Ocean Optics Protocols for Satellite Ocean Color Sensor Validation* revision 2 *NASA 98-107* (Greenbelt, MD: NASA Goddard Space Flight Center)

O'Reilly J E, Maritorena S, Mitchell B G, Siegel D A, Carder K L, Garver S A, Kahru M and McClain C 1998 Ocean color chlorophyll algorithms for SeaWiFS *J. Geophys. Res.* **103** 24937–53

O'Reilly J E *et al* 2000 Ocean color chlorophyll-a algorithms for SeaWiFS, OC2 and OC4 *SeaWiFS Postlaunch Calibration and Validation Analyses: Part 3* (*SeaWiFS Postlaunch Technical Report Series* vol 11) version 4, ed S B Hooker and E R Firestone (Greenbelt, MD: NASA Goddard Space Flight Center) pp 9–23

Ruddick K G, Ovidio F and Rijkeboer M 2000 Atmospheric correction of SeaWiFS imagery for turbid coastal and inland waters *Appl. Opt.* **39** 897–912

Sathyendranath S (ed) 2000 Remote sensing of ocean colour color in coastal and other optically complex waters *IOCCG Report* 3 Dartmouth, Nova Scotia

Sathyendranath S, Lazzara L and Prieur L 1987 Variations in the spectral values of specific absorption of phytoplankton *Limnol. Oceanogr.* **32** 403–15

Schiller H and Doerffer R 1999 Neural network for emulation of an inverse model—operational derivation of Case II water properties from MERIS data *Int. J. Remote Sens.* **20** 1735–46

Siegel D A and Michaels A F 1996 Quantification of non-algal light attenuation in the Sargasso Sea: implication for biogeochemistry and remote sensing *Deep-Sea Res.* 2 **43** 321–45

Siegel D A, Wang M H, Maritorena S and Robinson W 2000 Atmospheric correction of satellite ocean color imagery: the black pixel assumption *Appl. Opt.* **39** 3582–91

Tassan S and Ferrari G 1995 An alternative approach to absorption measurments of aquatic particles retained on filters *Limnol. Oceanogr.* **40** 1358–68

Tassan S and Ferrari G M 1998 Measurement of light absorption by aquatic particles retained on filters: determination of the optical pathlength amplification by the 'transmittance–reflectance' method *J. Plank. Res.* **20** 1699–709

Tassan S and Ferrari G M 2002 A sensitivity analysis of the 'transmittance–reflectance' method for measuring light absorption by aquatic particles *J. Plank. Res.* **24** 757–74

Tilstone G H, Moore G F, Sorensen K, Doerffer R, Rottgers R, Ruddick K G, Pasterkamp R and Jorgensen P V 2004a Regional validation of MERIS chlorophyll products in North Sea coastal waters: Protocols manual (Paris: European Space Agency) at press

Tilstone G H, Moore G F, Sorensen K, Doerffer R, Rottgers R, Jorgensen P V, Martinez Vicente V and Ruddick K G 2004b

Regional validation of MERIS chlorophyll products in North Sea coastal waters: inter-calibration report (Paris: European Space Agency) at press

Van der Linde D 1998 Protocol for total suspended matter *CEC-JRC Ispra (Technical Note)*

Van der Woerd 1999 Nordzee-atlas voor zwende stof *Rapport RIKZ/2001.013*

Vermote E F and Vermeulen A 1999 Atmospheric correction algorithm: spectral reflectance v.4 *MODIS ATBD 09* University of Maryland, USA

Warnock RE, Gieskes W W C and van Laar S 1999 Regional and seasonal differences in light absorption by yellow substance in the Southern Bight of the North Sea *J. Sea Res.* **42** 169–78

Wollast R 1998 Evaluation and comparison of the global carbon cycle in the coastal zone and in the open ocean *The Sea: The Global Coastal Ocean: Processes and Methods (Ideas and Observations on the Progress of the Study of the Seas* vol 10) ed K H Brink and A R Robinson (New York: Wiley) pp 213–52